Gene Therapy (2015) **22,** 578–590
© 2015 Macmillan Publishers Limited All rights reserved 0969-7128/15
www.nature.com/gt

ORIGINAL ARTICLE

Gene electrotransfer of plasmid AMEP, an integrin-targeted therapy, has antitumor and antiangiogenic action in murine B16 melanoma

M Bosnjak[1], T Dolinsek[1], M Cemazar[1,2], S Kranjc[1], T Blagus[1], B Markelc[1], M Stimac[1], J Zavrsnik[3], U Kamensek[1], L Heller[4], C Bouquet[5], B Turk[3] and G Sersa[1]

Gene therapy with Plasmid AMEP (antiangiogenic metargidin peptide) has recently been studied as a potential targeted therapy for melanoma. This plasmid is designed to downregulate α5β1 and αvβ3 integrins. In our study, electroporation was used as a nonviral delivery system. We investigated the antiangiogenic and direct antitumor effectiveness of this gene therapy on low and highly metastatic B16 melanoma variants. *In vitro*, the antiangiogenic effectiveness as determined by tube formation assay on endothelial cells was predominantly dependent on AMEP expression levels. *In vivo*, antitumor effectiveness was mediated by the inhibition of proliferation, migration and invasion of melanoma cells and correlated with the expression of integrins on tumor cells after intratumor delivery. In addition, reduced metastatic potential was shown. Intramuscular gene electrotransfer of Plasmid AMEP, for AMEP systemic distribution, had no antitumor effect with this specific preventive treatment protocol, confirming that direct tumor delivery was more effective. This study confirms our previous *in vitro* data that the expression levels of integrins on melanoma cells could be used as a biomarker for antitumor effectiveness in integrin-targeted therapies, whereas the expression levels of AMEP peptide could be a predictive factor for antiangiogenic effectiveness of Plasmid AMEP in the treatment of melanoma.

Gene Therapy (2015) **22,** 578–590; doi:10.1038/gt.2015.26

INTRODUCTION

Among the new molecular targeted approaches for melanoma treatment, gene therapy approaches have been demonstrated to be safe and effective.[1] Gene electrotransfer (GET) of a plasmid encoding interleukin-12 directly to melanoma nodules was demonstrated in a clinical trial to be effective on the treated nodules as well as on nontreated in transit melanoma metastases.[2,3] GET could therefore be used for safe and effective targeted therapy of melanoma using different therapeutic plasmids.

In normal and tumor cells, binding of extracellular matrix proteins to integrins leads to changes in cell attachment, intracellular signaling and gene expression thereby controlling cell differentiation, proliferation, migration and survival.[4] Many integrins are overexpressed in different types of cancers, which consequently results in aberrant cell signaling and increased proliferation and migration. AMEP (antiangiogenic metargidin peptide) is an integrin receptor antagonist that moderates aberrant cell signaling of integrins α5β1 and αvβ3, which are overexpressed in melanoma tumor cells and active endothelial cells involved in angiogenesis. Thus, this peptide has a dual, antitumor and antiangiogenic effect.

For the treatment of melanoma, a recombinant disintegrin domain of metargidin (RDD) was previously demonstrated to have antiangiogenic and antitumor effectiveness *in vitro*, using a recombinant protein, and *in vivo* using RDD-coding plasmids.[5,6] On the basis of these observations, Plasmid AMEP, a plasmid DNA devoid of any antibiotic resistance gene and coding for AMEP peptide (equivalent to RDD) under the control of the cytomegalovirus promoter, was constructed.

Plasmid AMEP was previously tested *in vitro* and has antiproliferative and antimetastatic effects in murine melanoma cells and a strong antiangiogenic effect in human endothelial cell lines.[7] In addition, intratumoral GET of Plasmid AMEP was previously tested in a Phase I clinical trial as a new therapeutic approach for treatment of malignant melanoma. Plasmid AMEP delivery was well tolerated with local antitumor effectiveness in treated lesions observed, whereas no related severe adverse effects were noted.[8] Phase I/II studies were then launched, which were aimed at delivering Plasmid AMEP intramuscularly, so as to exert a systemic therapy to multiple metastases (www.clinicaltrial.gov).

Although Plasmid AMEP has been tested in initial clinical trials, solid preclinical data on evaluation of its mechanisms of action and predictive factors for response to treatment are still needed. Our *in vitro* study indicated that the expression of integrins on melanoma cells could be a biomarker for the antitumor effectiveness of integrin-targeted therapies, whereas the expression levels of AMEP peptide could be a predictive factor for its antiangiogenic effect.[7] No *in vivo* preclinical data are yet available to confirm this hypothesis.

Therefore, in the current study, we present the *in vivo* effect of Plasmid AMEP in melanoma in mice. Data on antitumor effectiveness after intratumoral or intramuscular GET of Plasmid

[1]Department of Experimental Oncology, Institute of Oncology Ljubljana, Zaloska 2, Ljubljana, Slovenia; [2]Faculty of Health Sciences, University of Primorska, Polje 42, Izola, Slovenia; [3]Department of Biochemistry and Molecular and Structural Biology, Jozef Stefan Institute, Jamova cesta 39, Ljubljana, Slovenia; [4]Frank Reidy Research Center for Bioelectrics, Old Dominion University, 4211 Monarch Way, Norfolk, Virginia, USA and [5]ONXEO, Boulevard du Général Martial Valin 49, Paris, France. Correspondence: Professor G Sersa, Department of Experimental Oncology, Institute of Oncology Ljubljana, Zaloska 2, Ljubljana SI-1000, Slovenia.
E-mail: gsersa@onko-i.si
Received 3 November 2014; revised 3 February 2015; accepted 9 March 2015; accepted article preview online 17 March 2015; advance online publication, 9 April 2015

AMEP are presented on low- and high-metastatic melanoma variants B16F1 and B16F10. The antitumor effectiveness was studied also by histological analysis of tumor sections, evaluating proliferation, necrosis, apoptosis of tumor cells and enumerating tumor blood vessels. Furthermore, the antiangiogenic effectiveness was evaluated *in vitro* and *in vivo* in a dorsal window chamber model. In addition, reduced antimetastatic potential of treated tumors was shown after GET of Plasmid AMEP. These *in vivo* data confirm our previous *in vitro* data and demonstrate that the expression of integrins on melanoma cells could serve as a biomarker for antitumor effectiveness of integrin-targeted therapies, whereas intratumoral expression levels of AMEP peptide could serve as a predictive factor for its antiangiogenic effectiveness.

RESULTS

Antiangiogenic effects of Plasmid AMEP on murine endothelial cells *in vitro*

The antiangiogenic effects of Plasmid AMEP were first evaluated *in vitro* in murine SVEC 4–10 endothelial cell line by proliferation, adhesion, migration, invasion and tube formation assays.

GET of Plasmid AMEP (10 μg) significantly reduced the proliferation of cells (Figure 1a). At day 4, the proliferation of endothelial cells was significantly reduced to ~70%. GET of pEGFP (enhanced green fluorescent protein, 10 μg), a control plasmid, did not affect cell proliferation. In a model mimicking the tumor environment, adhesion ability of SVEC 4–10 cells on basement membrane matrix Matrigel was not affected after GET of Plasmid AMEP (Figure 1b). However, the migration and invasion of endothelial cells were significantly reduced after the treatment by ~40% and 65%, respectively (Figures 1c and d), whereas the control plasmid pEGFP (10 μg) had no effect.

The antiangiogenic effectiveness of Plasmid AMEP delivery *in vitro* was supported by tube formation assay. Formation of capillary-like structures *in vitro* was minimally (nonstatistically) reduced 1 day after GET of Plasmid AMEP (Figure 2). AMEP mRNA levels (Table 1) were higher in the Plasmid AMEP GET group than in the control group, but less elevated than the levels observed in our previous study on human endothelial cells.[7] This could be explained by different electroporation-mediated transfection efficiency between the cell types used. Despite the optimization of different pulse parameters,[9,10] it is indeed difficult to achieve high transfection efficiency of SVEC 4–10 cells with GET *in vitro*. Therefore, we additionally transfected SVEC 4–10 cells with Plasmid AMEP using lipofectamine as transfection reagent in order to confirm the dose-dependent antiangiogenic effect previously observed.[7] Formation of capillary-like structures after lipofectamine transfection of SVEC 4–10 cells with Plasmid AMEP (2 μg) was completely reduced (Figure 2). This strong effect was correlated to a higher expression of AMEP compared with the expression after GET. Higher levels of AMEP mRNA resulted in statistically significant higher number of tubular complexes (Figure 2, Table 1).

Antitumor effects after intratumoral GET of Plasmid AMEP *in vivo*

The antitumor effectiveness of Plasmid AMEP *in vivo* was tested on two subcutaneous B16F1 and B16F10 melanoma models with low and high metastatic potential, respectively. When tumors had a diameter of 3 mm (day 0), GET was done. The procedure was repeated on day 2. Intratumoral GET of Plasmid AMEP resulted in statistically significant antitumor effectiveness in both melanoma models; the tumor growth delay to reach 40 mm^3 volume was similar in both tumor models (Figure 3), that is, 9.4 ± 0.9 days in B16F1 and 8.7 ± 1.1 days in B16F10 tumors (Table 2). Most importantly, complete response was observed after intratumoral GET of Plasmid AMEP with 17% and 35% of completely regressed tumors in the B16F1 and B16F10 models, respectively (Table 2). GET of the control blank plasmid pControl also resulted in a significant growth delay compared with untreated control tumors in both tumor models; however, this growth delay was statistically significantly shorter than the one induced by GET of Plasmid AMEP.

In order to confirm the results of our previous *in vitro* study, intratumor AMEP mRNA expression levels were determined 5 days after GET of Plasmid AMEP *in vivo* in both melanoma models. The quantitative reverse transcription-PCR (qRT-PCR) analysis showed significantly higher AMEP mRNA levels in both melanoma models after GET of Plasmid AMEP in comparison with control. No statistically significant changes in AMEP mRNA expression levels were observed in other groups compared with the untreated control tumors. The average expression level of AMEP mRNA in B16F10 melanoma was up to 10-fold higher than in B16F1 tumor model (Table 2), which confirmed our *in vitro* data in murine melanoma cells.[7]

Histological analysis of tumor sections after intratumoral GET of Plasmid AMEP

The antitumor effectiveness was also evaluated by the induction of tumor necrosis and apoptosis as well as the reduction of cell proliferation in the viable tumor tissue. Hematoxylin and eosin staining of tumor sections showed statistically significant increased proportion of necrosis in Plasmid AMEP-treated tumors in both melanoma models, without any difference between them (Figure 4a). The untreated tumors had ~30% necrosis, whereas the tumors treated with GET of Plasmid AMEP had ~80% necrosis, which was evenly distributed throughout the tumor tissue.

There was no clear sharp boundary between necrotic and viable tissue and so the proportion of apoptotic cells was evaluated in both areas. The proportion of apoptotic cells was significantly increased in the B16F1 tumor model, whereas in B16F10 the increase was minimal and nonsignificant (Figure 4b). Cell proliferation was also assessed in the viable areas of tumor tissue. The proportion of proliferating cells was decreased by ~60% in GET plasmid AMEP treated tumors compared with control untreated tumors (Figure 5), regardless of the tumor model.

Effects of intramuscular GET of Plasmid AMEP on tumor outgrowth and growth

Intramuscular GET of Plasmid AMEP was performed in a tumor B16F1 model to test the possible systemic antitumor effectiveness of circulating AMEP peptide on distant subcutaneous tumors, with our preventive treatment protocol (at days −3 and −1). Tumor outgrowth test for a possible direct antiangiogenic effect and tumor growth delay were assessed for antitumor effectiveness. Deliveries were performed on B16F1 tumors with two different doses of Plasmid AMEP (50 or 200 μg) on days −3 and −1 before tumor induction. No statistically significant effect ($P = 0.998$ between groups) on outgrowth and growth of tumors was detected, indicating that circulating AMEP peptide may not have an effect on distant tumors or metastases (Figure 6).

Antiangiogenic effects of Plasmid AMEP *in vivo*

The *in vivo* antiangiogenic effects of intratumoral Plasmid AMEP GET were evaluated by CD31 immunostaining of blood vessels in tumor sections and by intravital microscopy in dorsal window chamber model.

Immunohistological staining of B16F1 and B16F10 tumor sections for CD31 endothelial marker demonstrated a strong antiangiogenic effect of Plasmid AMEP GET. The number of tumor blood vessels was significantly reduced after treatment and reached 30% of the untreated control groups in both tumor

© 2015 Macmillan Publishers Limited

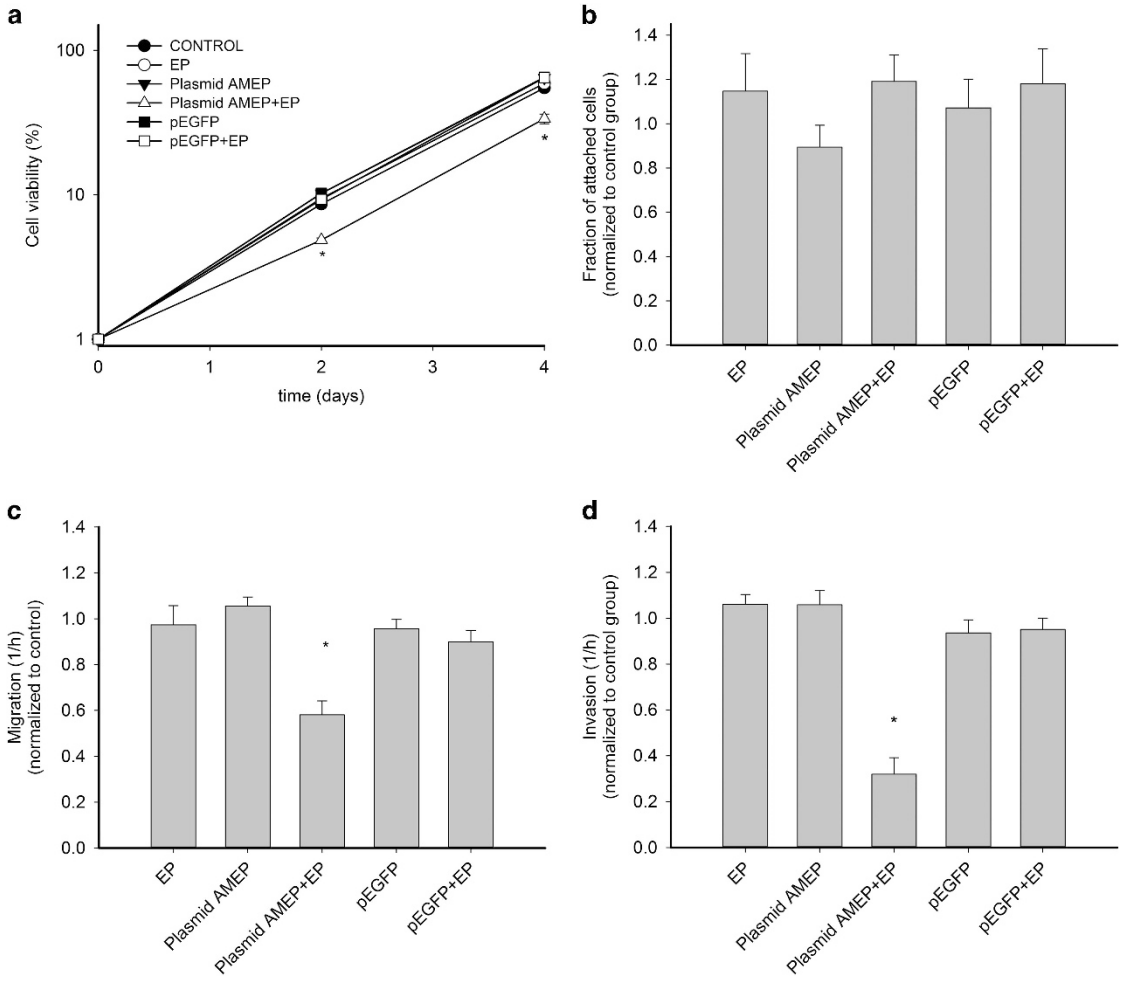

Figure 1. GET of Plasmid AMEP reduced proliferation (**a**), migration (**c**) and invasion (**d**) but not cell adhesion (**b**) of murine SVEC 4–10 endothelial cells. Cells were transfected with 10 μg of pEGFP or Plasmid AMEP with or without electroporation (EP). Proliferation of cells in each experimental group was normalized to day 0. Adhesion, migration and invasion of SVEC 4–10 cells in each experimental group were normalized to the untreated control group. $^*P < 0.05$ vs all groups. Results represent three independent experiments, $n = 6$ for each experimental group in each experiment, and are expressed as mean ± s.e.

models (Figure 7), indicating a reduction in blood vessel formation.

The antiangiogenic effect of Plasmid AMEP was further investigated in a dorsal window chamber model for direct observation of tumor blood vessels.

Angiogenesis in B16F1 control tumors was continuous, forming a chaotic vascular network. GET of Plasmid AMEP resulted in the complete prevention of the formation of new tumor blood vessels from the first day after the treatment. This was confirmed by visualization of the functional vessels in the tumors using FITC (fluorescein isothiocyanate)-labelled dextran, which was intravenously injected into mice on day 5 after therapy (Figure 8). Owing to the abrogated blood flow, treated tumor size remained unchanged, whereas all the control tumors continuously grew in a time frame from day 1 to day 5 (Figure 8). Those tumors displayed functional blood vessels at day 5, which were observed after FITC dextran injection (Figure 8).

The same antiangiogenic effect of GET Plasmid AMEP was observed in B16F10 melanoma. However, due to its high melanin content, it was harder to follow vessel formation and to monitor the antiangiogenic effects. Therefore, we used two different florescent labels that enabled the identification of functional blood vessels on two consecutive days (FITC dextran on day 3 and Rhodamine B on day 4; Figure 9). Tumor treatment with Plasmid AMEP GET completely abrogated the formation of tumor blood vessels in B16F10 tumors, whereas it did not affect the surrounding normal vessels. Tumor growth and the formation of blood vessels were not affected in the control groups.

Plasmid AMEP affects integrin signaling pathway *in vivo*

In order to confirm the cellular pathway of Plasmid AMEP action, we performed analysis of mRNA levels in the integrin-linked signaling pathway after a single treatment with GET of Plasmid AMEP by evaluating talin, vinculin, integrin-linked kinase, Rac and cSrc. Talin is the first effector protein following α5β1 integrin, whereas vinculin, integrin-linked kinase, Rac and cSRC are involved in cell proliferation, migration and invasion. Rac and cSRC are also involved in the crosstalk between the αvβ3 integrin and the VEGF-A/VEGFR2 angiogenesis signaling pathway. A nonsignificant decrease in mRNA levels in experimental and control groups was observed 24 h after delivery (Table 3). No inhibitory effects were observed 4 or 60 h after delivery (data not shown).

Plasmid AMEP effect on metastatic potential

To confirm the antimetastatic potential of Plasmid AMEP GET suggested *in vitro*,[7] an experiment was performed with highly

© 2015 Macmillan Publishers Limited

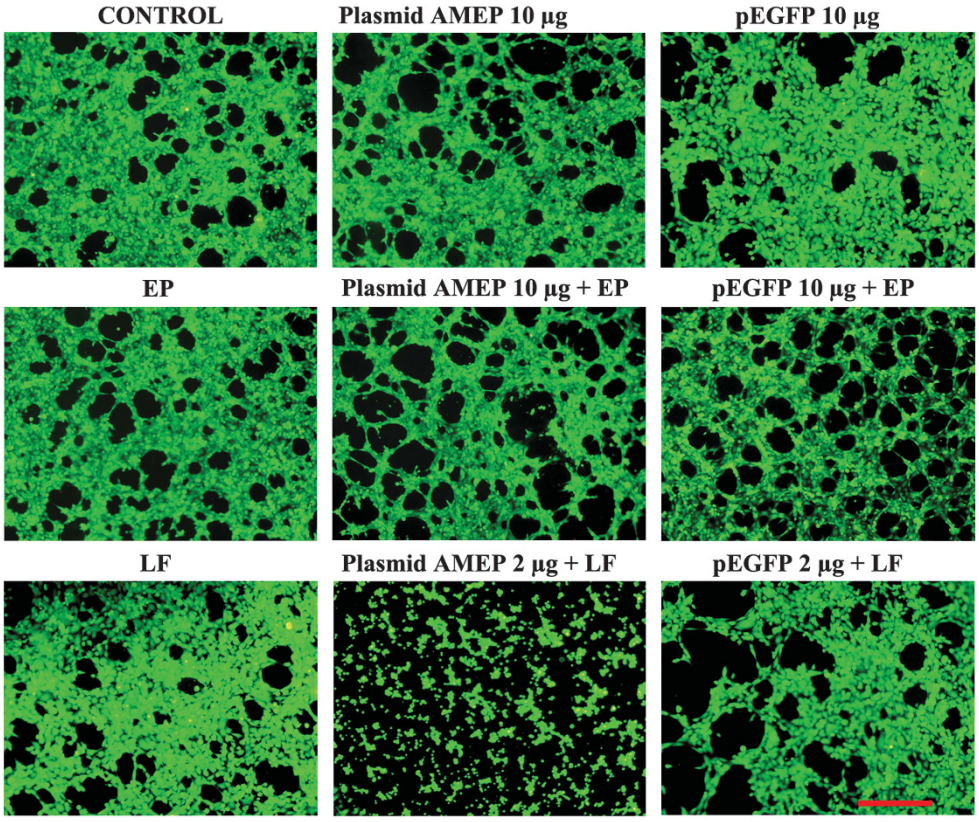

Figure 2. Plasmid AMEP reduced the tube formation of SVEC 4–10 endothelial cells after lipofection (LF), but not after GET. Original images of tubular complexes after GET and LF of Plasmid AMEP and corresponding control groups. Scale bar, 500 µm.

Table 1. Fold expression of AMEP mRNA in murine endothelial SVEC 4–10 cell line after EP or lipofection LF of Plasmid AMEP and corresponding number of tubular complexes (normalized to control untreated group) formed in tube formation assay

Group	*Fold expression of AMEP mRNA*	*Number of tubular complexes (normalized to control group)*
Control	1.00 ± 0.00	1.00 ± 0.03
EP	0.82 ± 0.51	0.89 ± 0.33
Plasmid AMEP 10 µg	2.49 ± 1.86	0.79 ± 0.09
Plasmid AMEP 10 µg+EP	22.01 ± 11.17*	2.61 ± 1.06
pEGFP 10 µg	1.71 ± 0.08	0.86 ± 0.43
pEGFP 10 µg+EP	1.74 ± 0.12	1.07 ± 0.21
Lipofectamine (LF)	0.90 ± 0.58	1.24 ± 0.53
Plasmid AMEP 2 µg+LF	2 894.11 ± 255.16*	52.00 ± 11.29*
pEGFP 2 µg+LF	1.01 ± 0.19	0.71 ± 0.01

Abbreviations: AMEP, antiangiogenic metargidin peptide; EGFP, enhanced green fluorescent protein; EP, electroporation; LF, lipofectamine. Values represent mean ± s.e. *$P < 0.05$ compared with all groups. Results represent three independent experiments, $n = 4$ for each experimental group in each experiment.

metastatic B16F10 tumors. Treated subcutaneous tumors were excised 3 days after the second treatment and the mice were monitored for the development of distant metastases. The metastases were most commonly localized in lymph nodes (on the side of tumor implantation) or in the lungs. The data suggest that GET of Plasmid AMEP decreased metastatic potential of B16F10 tumors, as the mice after the treatment developed significantly fewer distant metastases (Figure 10, Table 4).

DISCUSSION

Gene therapy using Plasmid AMEP has direct antitumor and antiangiogenic effect on melanoma tumors. AMEP acts through the inhibition of integrin-linked signaling pathway as confirmed in our study. The antitumor effectiveness of Plasmid AMEP on melanoma cells is mediated by the inhibition of their proliferation, migration and invasion, which correlates with the expression of integrins on tumor cells.[7] The importance of this biomarker as a predictive factor for the response to treatment was indicated in our previous study, where we observed the correlation of biological effect with the integrin quantity on the cells and not with the expression levels of AMEP after GET with Plasmid AMEP,[7] and confirmed in this first *in vivo* study in the B16F1 and B16F10 melanoma tumor models. The antiangiogenic effectiveness of intratumoral GET with Plasmid AMEP is specific for activated endothelial cells. Its contribution to overall antitumor effectiveness

© 2015 Macmillan Publishers Limited

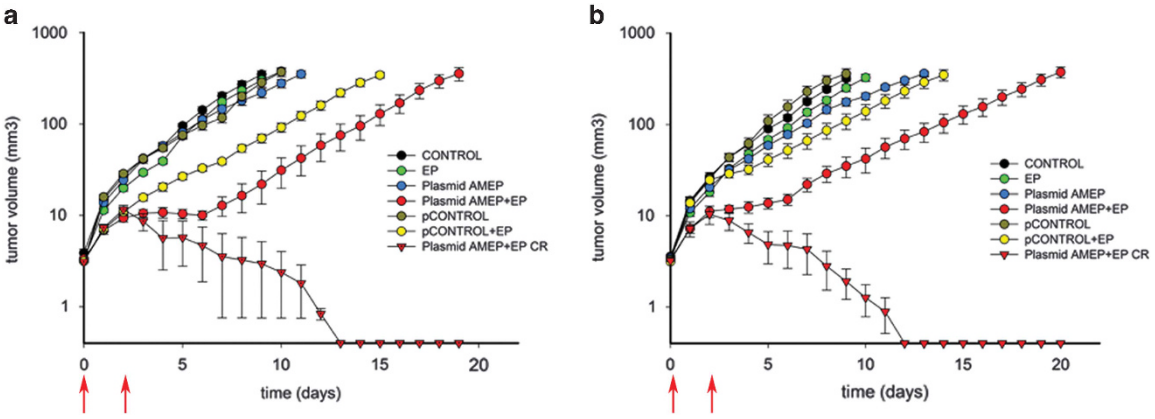

Figure 3. Two repeated intratumoral GET of Plasmid AMEP reduced the growth of B16F1 and B16F10 melanoma tumors. Growth of B16F1 (**a**) and B16F10 (**b**) melanoma tumors after two intratumoral GET of pControl plasmid or Plasmid AMEP (100 μg) at days 0 and 2. In B16F1 tumor model (**a**) a complete response (CR, Plasmid AMEP+EP CR) was observed in 3 out of 18 mice after GET of Plasmid AMEP, whereas other 15 mice responded with delayed tumor growth (Plasmid AMEP+EP). In B16F10 tumor model (**b**) there was a CR (Plasmid AMEP+EP CR) in 7 out of 18 mice after GET of Plasmid AMEP, whereas other 11 mice responded with delayed tumor growth (Plasmid AMEP+EP). Arrows indicate days of treatment. Results represent two independent experiments, $n = 6–9$ for each experimental group in each experiment, and are expressed as mean ± s.e.

is substantial, and likely contributes to the complete tumor eradication observed in this study. Expression levels of AMEP peptide could be a predictive factor for antiangiogenic effectiveness of this melanoma treatment. The reduced antimetastatic potential of melanoma tumor cells after GET of Plasmid AMEP could substantially contribute to the overall effectiveness of the therapy and lower the risk of tumor recurrence. However, intramuscular GET of Plasmid AMEP according to the applied treatment schedule does not provide therapeutic effectiveness, which may be due to the short half-life or biodegradation of the peptide in the circulation. Although the expression levels of AMEP after intramuscular GET were not determined, the efficient transfection was confirmed with GET of pEGFP in our previous experiments.[11]

The effects of AMEP were first demonstrated in a study evaluating the effects of RDD (also named AMEP) *in vitro* as a recombinant protein and *in vivo* as a plasmid coding for RDD containing an antibiotic-resistance gene.[5] This study demonstrated the antitumor effectiveness of RDD encoding inducible plasmid after intramuscular GET in the MDA-MB-231 breast tumor model and the antimetastatic potential on the B16F10 melanoma tumor model in mice. The antiangiogenic effect was also shown *in vivo* as confirmed by anti-CD31 staining of tumor sections.[5] Another study in melanoma B16F10 tumor model confirmed the antitumor and antimetastatic effectiveness of a plasmid coding for RDD after intratumoral transfection.[6] Plasmid AMEP was also tested *in vitro* with significant antiangiogenic effectiveness. In addition, its antiproliferative and antimetastatic effects were shown *in vitro* on melanoma cell lines.[7]

Electroporation was used as a delivery system, as it is safe and effective for the introduction of small molecules, such as bleomycin or cisplatin,[12–22] as well as larger molecules, such as plasmid DNA or small noncoding RNA.[7,23–30] In a recent study, it was shown that GET of Plasmid AMEP in a combined modality treatment with radiation had a radiosensitizing effect based on the normalization of tumor vasculature and consequently on improved tumor oxygenation.[31] These data support our data on antiangiogenic effectiveness of Plasmid AMEP GET.

On the basis of the RDD data,[5] the first clinical Phase I/II study with intratumoral Plasmid AMEP administration was conducted. This study was unique in that the Plasmid AMEP was devoid of any antibiotic-resistance gene. The clinical study on five patients treated with Plasmid AMEP intratumoral gene electrotransfered demonstrated good tolerability of Plasmid AMEP, local antitumor effectiveness in the treated lesions and no related severe adverse events.[8]

In our study, the antitumor effectiveness *in vivo* was very similar in both metastatic and non-metastatic melanoma models with no significant difference in tumor growth delay between the tumor models observed. However, tumor mRNA levels after GET of Plasmid AMEP were almost 10-fold higher in the highly metastatic B16F10 tumor model, indicating that AMEP mRNA expression levels did not correlate with the biological effect, suggesting that even a low level of AMEP expression is sufficient to delay tumor growth in the models. This same observation was made in our previous study *in vitro* in murine melanoma cells.[7] Histological staining of tumor sections from both tumor models showed an increased proportion of necrosis and apoptosis as well as decreased proliferation of viable regions/areas. The data suggest that the antitumor effect is most probably driven by a direct antiproliferative and cytotoxic effect and also by an antimetastatic (for B16F10 tumor model) effect of Plasmid AMEP to melanoma cells. The same effects were observed on B16F1 and B16F10 cells in our *in vitro* study.[7]

Antiangiogenic effect may be a result of two main factors which are linked: the integrin quantity on endothelial cells and also the expression levels of AMEP. As shown previously on human endothelial cells,[7] we confirmed here on murine endothelial SVEC 4–10 cells that even a low expression level of AMEP inhibited proliferation, migration and invasion of endothelial cells, whereas high expression levels of AMEP were needed for reduction of the formation of capillary-like structures.

The antiangiogenic activity of Plasmid AMEP GET *in vivo* was first demonstrated by staining tumor sections for the CD31 endothelial cell marker, where a significant reduction of the blood vessels was observed. In addition, HE staining showed that tumor necrosis was not centralized, but was evenly distributed over the tumor. This indicates that the vascular action of Plasmid AMEP is based on antiangiogenic and not vascular disrupting activity, where, most commonly, central necrosis with viable tumor rim is observed. Plasmid AMEP expression thus prevents the formation of new tumor blood vessels and this effect is visible throughout the entire tumor. Furthermore, the inhibited formation of tumor blood vessels was confirmed in a dorsal window chamber model. In all control groups, the new vessels were formed continuously after tumor implantation, whereas in the group receiving GET of

© 2015 Macmillan Publishers Limited

Table 2. Growth delay, CR and fold expression of AMEP mRNA in B16F1 and B16F10 tumors 3 days after second intratumoral GET of Plasmid AMEP

Group	*Tumor growth delay (days)*	*N (%) of CR*	*Fold expression of AMEP mRNA*
B16F1 tumors			
Control		0	1.0 ± 0.0
EP	0.71 ± 0.14	0	1.3 ± 0.4
Plasmid AMEP	0.40 ± 0.40	0	16.4 ± 5.4
Plasmid AMEP+EP	9.36 ± 0.85*	3/18 (17)*	44 113.2 ± 22 985.6*
pControl	−0.23 ± 0.24	0	2.0 ± 1.1
pControl+EP	4.11 ± 0.50	0	24.1 ± 23.5
B16F10 tumors			
Control		0	1.0 ± 0.0
EP	0.68 ± 0.20	0	7.4 ± 6.7
Plasmid AMEP	0.93 ± 0.25	0	18.1 ± 13.2
Plasmid AMEP+EP	8.70 ± 1.13*	7/18 (35)*	303 820.1 ± 297 480.1*
pControl	0.03 ± 0.28	0	3.3 ± 1.6
pControl+EP	4.57 ± 1.50	0	41.8 ± 35.5

Abbreviations: AMEP, antiangiogenic metargidin peptide; CR, complete response; EP, electroporation; GET, gene electrotransfer. *$P < 0.05$ compared with all groups; number of mice in each group = 12–18. Mice that were tumor free (CR) were excluded from the calculations of tumor growth delay. Values represent mean ± s.e.

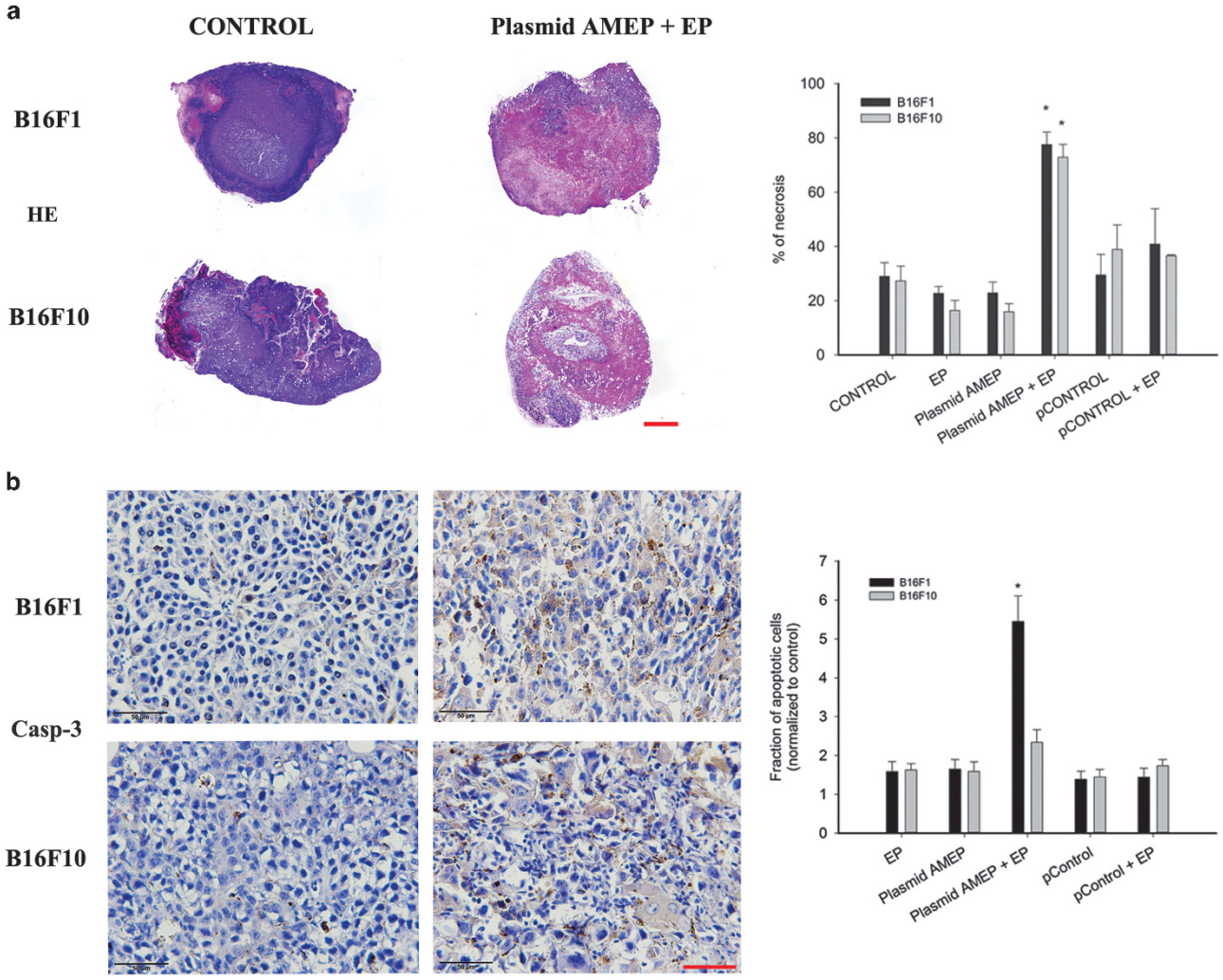

Figure 4. Two repeated intratumoral GET of Plasmid AMEP increased necrosis (HE) in B16F1 and B16F10 tumors (**a**), and apoptosis (Casp-3) in B16F1 (**b**). Scale bar, 1 mm (**a**) and 50 μm (**b**). Results represent two independent experiments, $n = 2$ for each experimental group in each experiment, and are expressed as mean ± s.e. *$P < 0.05$ vs all groups.

© 2015 Macmillan Publishers Limited

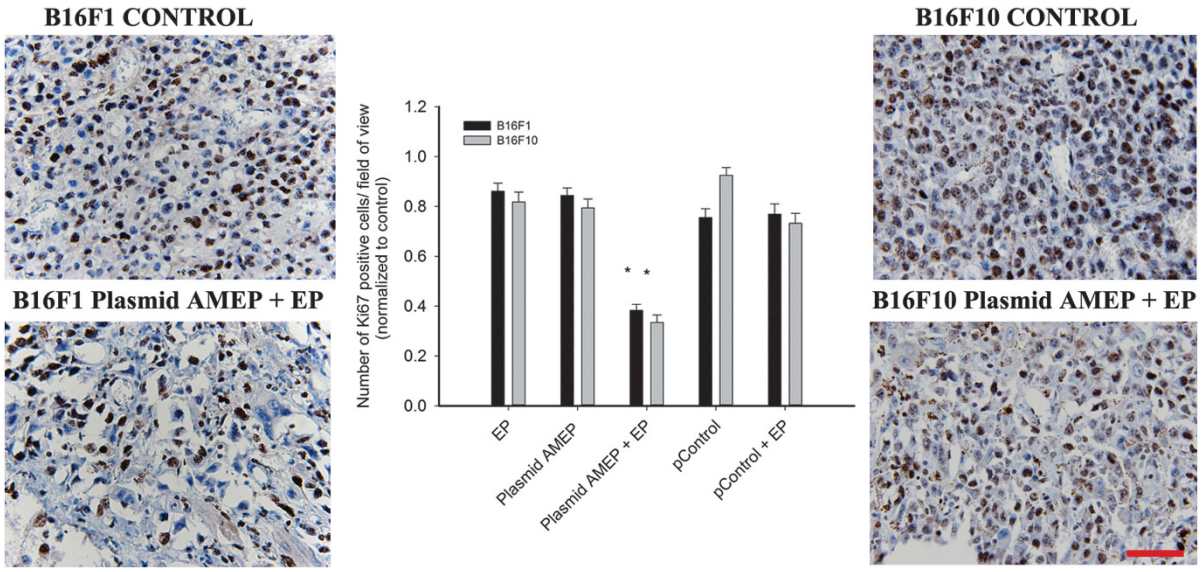

Figure 5. Two repeated intratumoral GET of Plasmid AMEP reduced the proliferation of tumor cells (Ki67 staining) in viable parts of B16F1 and B16F10 tumors. Scale bar, 50 μm. Results represent two independent experiments, $n = 2$ for each experimental group in each experiment, and are expressed as mean ± s.e. $^*P < 0.05$ vs all groups.

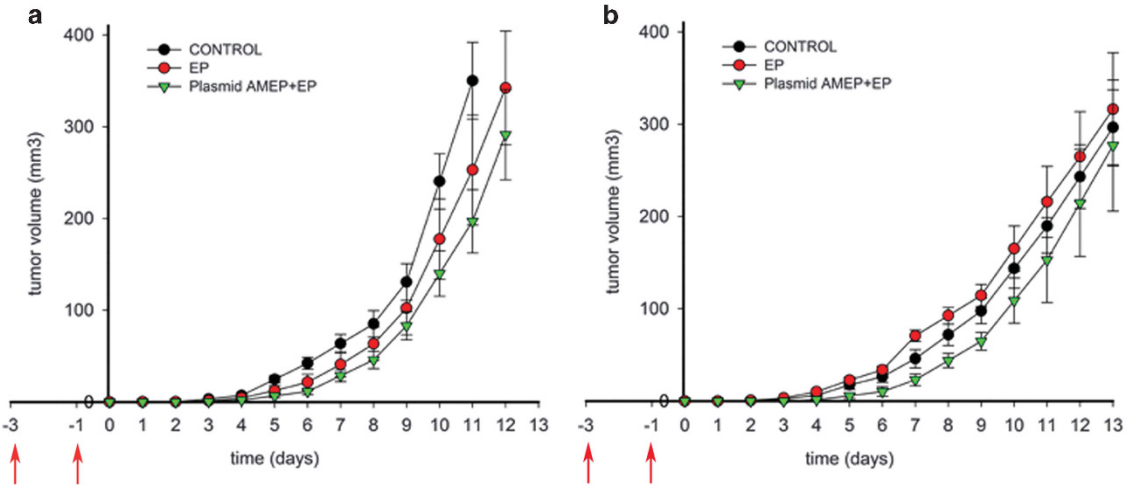

Figure 6. Repeated intramuscular GET of Plasmid AMEP before tumor implantation (day 0) had no effect on outgrowth and growth of B16F1 melanoma tumors. Outgrowth and growth of B16F1 murine melanoma model after two intramuscular GET of Plasmid AMEP 50 μg (**a**) or Plasmid AMEP 200 μg (**b**). Arrows indicate days of treatment. Results represent two independent experiments, $n = 6$ for each experimental group in each experiment and are expressed as mean ± s.e.

Plasmid AMEP, no new blood vessel formation was observed after the therapy. This observation suggests a strong antiangiogenic effect after GET of Plasmid AMEP, which could also have impact on VEGF signaling, as there crosstalk with integrin signaling pathways is well established, especially because there was no normalization (sprouting of new vessels) around the tumor.[32]

To determine the overall effectiveness of the therapy, the intratumoral AMEP levels should be evaluated as we know that higher levels of AMEP contributed to a stronger antiangiogenic effect, which, in combination with the antitumor effect, could result in complete tumor eradication. Antiangiogenic agents alone rarely completely inhibit tumor growth; therefore, their therapeutic use is mainly in combination with other antitumor agents. Owing to this, Plasmid AMEP with its dual action represents a good therapeutic approach, especially in tumors with high expression levels of AMEP peptide, like here in B16F10 murine melanoma model, where GET of Plasmid AMEP could induce complete response.

Recently, clinical trials on intramuscular Plasmid AMEP were initiated as Phase I/II studies (NCT01664273; NCT01764009). The rationale of these trials was not based on published data; therefore, we assessed Plasmid AMEP effectiveness when electrotransfered intramuscularly, in order to evaluate distant effects by blood circulation of the AMEP peptide. Although the localized or systemic plasmid expression *in vivo* was not confirmed after intramuscular delivery, our data do not support the concept of systemic antitumor effectiveness. The experiments with two doses of Plasmid AMEP GET to muscle at days −3 and −1 before tumor implantation, with very high quantity of plasmid, had no effect on tumor outgrowth or subsequent transition from avascular to

© 2015 Macmillan Publishers Limited

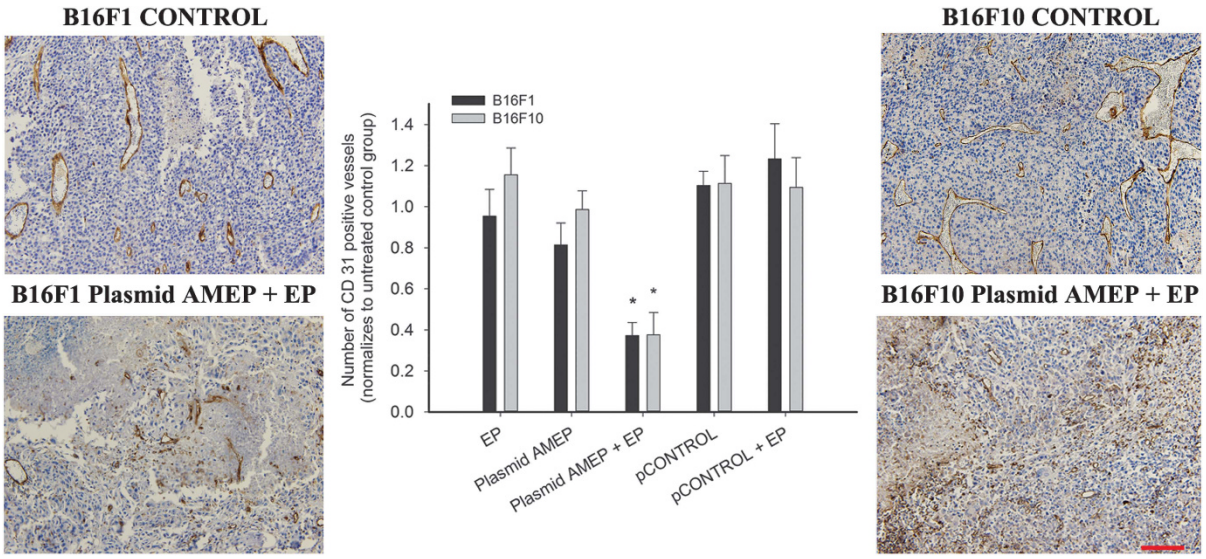

Figure 7. Two intratumoral GETs of Plasmid AMEP reduced number of vessels (anti-CD31 staining) in viable parts of B16F1 and B16F10 tumors. Scale bar, 200 μm. Results represent two independent experiments, $n = 2$ for each experimental group in each experiment, and are expressed as mean ± s.e. $^*P < 0.05$ vs all groups.

vascular phase of tumor growth. The specific transfection protocol used in our previous study was already shown to be very efficient for the transfection of plasmid encoding IL-12.[3,11] However, we cannot exclude the possibility that other protocols might prove more effective, with modulating treatment schedules or plasmid doses.

In summary, GET of Plasmid AMEP is an effective method for the local treatment of murine melanoma tumors, where the overall effect is a consequence of the intertwined antitumor and antiangiogenic action of AMEP factor. In antitumor effectiveness, the key factor is the quantity of integrins on tumor cells, resulting in growth delay, whereas in antiangiogenic effect also the expression levels of AMEP are important. If the expression levels of AMEP therapeutic peptide are sufficient, a very strong antiangiogenic effect occurs, which, in combination with the direct antitumor effect can lead to a total tumor regression. Indeed, we demonstrated the increased number of complete tumor regressions in the B16F10 tumor model where a higher expression of AMEP mRNA was achieved. The reduced anti-metastatic potential of melanoma tumor cells after GET of Plasmid AMEP may lower the risk of tumor recurrence and thus substantially contribute to the overall effectiveness of gene therapy with Plasmid AMEP.

MATERIALS AND METHODS

Cell lines

Murine melanoma cell lines; B16F1 with low metastatic potential and B16F10 with high metastatic potential (American Type Culture Collection, Manassas, VA, USA) or B16-F10-luc-G5 (PerkinElmer, Waltham, MA, USA) were cultured in advanced minimum essential medium (Life Technologies, Carlsbad, CA, USA) supplemented with 5% fetal bovine serum (FBS, Life Technologies), 10 mM/l L-glutamine (Life Technologies), 100 U ml^{-1} penicillin (Grünenthal, Aachen, DE) and 50 mg ml^{-1} gentamicin (Krka, Novo mesto, Slovenia) in a 5% CO_2 humidified incubator at 37 °C.

Murine endothelial cell line SVEC 4–10 (American Type Culture Collection) was cultured in advanced Dulbecco's modified eagle medium (Life Technologies) supplemented with 5% FBS, 10 mM l^{-1} L-glutamine, 100 U ml^{-1} penicillin and 50 mg ml^{-1} gentamicin in a 5% CO_2 humidified incubator at 37 °C.

Plasmids

Plasmid AMEP (ONXEO) is a 2.5-kb therapeutic plasmid consisting of an expression cassette for AMEP inserted in a plasmid backbone devoid of any antibiotic resistance gene (ORT Technology, Cobra Biologics, Keele, UK). The AMEP transgene is a fusion between the sequences encoding the secretion signal peptide from human urokinase and the human AMEP and is placed downstream of the human cytomegalovirus CMV-intron A enhancer/promoter and upstream to the late bovine growth hormone polyadenylation signal.[7] Each vial of Plasmid AMEP was reconstituted in 500 μl of endotoxin-free water. The plasmid concentration of 4 mg ml^{-1} was immediately used for *in vivo* experiments. For *in vitro* experiments, plasmid was further diluted to 1 or 2 mg ml^{-1}.

Plasmid DNA encoding eGFP under the control of the CMV promoter, CMV-EGFP-N1 (pEGFP, BD Biosciences Clontech, Palo Alto, CA, USA) and pControl, without the eGFP insert, were used as control plasmids. pControl (see Supplementary Figure) was used in *in vivo* experiments in order to avoid the interference of eGFP fluorescence to further analysis. Control plasmids were amplified in competent *Escherichia coli* and then isolated and purified with JetStar Plasmid Purification Kit (Genomed, Leesburg FL, USA) according to the manufacturer's protocol. Quality and quantity of isolated plasmids were determined by spectrophotometric method (Epoch Microplate Spectrophotometer, Take3 Micro-Volume Plate, BioTek, Bad Friedrichshall, Germany) and agarose gel electrophoresis. pEGFP was diluted in endotoxin-free water to a final concentration of 1, 2 or 4 mg ml^{-1}, whereas the concentration of pControl was 4 mg ml^{-1}.

In vitro GET of plasmid DNA

A monolayer of 80% confluent SVEC 4–10 cells was trypsinized, washed with corresponding media and washed again in ice-cold electroporation buffer (EP buffer: 125 mM sucrose; 10 mM K_2HPO_4; 2.5 mM KH_2PO_4; 2 mM $MgCl_2{\cdot}6H_20$). For EGT, a cell suspension (25×10^6 cells ml^{-1}) was prepared in ice-cold EP buffer. Several aliquots of 44 μl were prepared and before the electroporation 11 μl of different plasmids (pEGFP, Plasmid AMEP) or endotoxin-free water were added. Fifty μl of the resulting mixture, containing 1×10^6 cells, wase pipetted between two parallel stainless-steel plate electrodes with a 2-mm gap in-between. Eight square wave electric pulses (EP), with voltage-to-distance ratio 600 V cm^{-1}, pulse duration 5 ms and frequency 1 Hz were generated by electric pulse generator GT-01 (Faculty of Electrical Engineering, University of Ljubljana, Slovenia). Cells were incubated for 5 min in 100 μl of FBS and then plated in the appropriate medium for further assays.

© 2015 Macmillan Publishers Limited

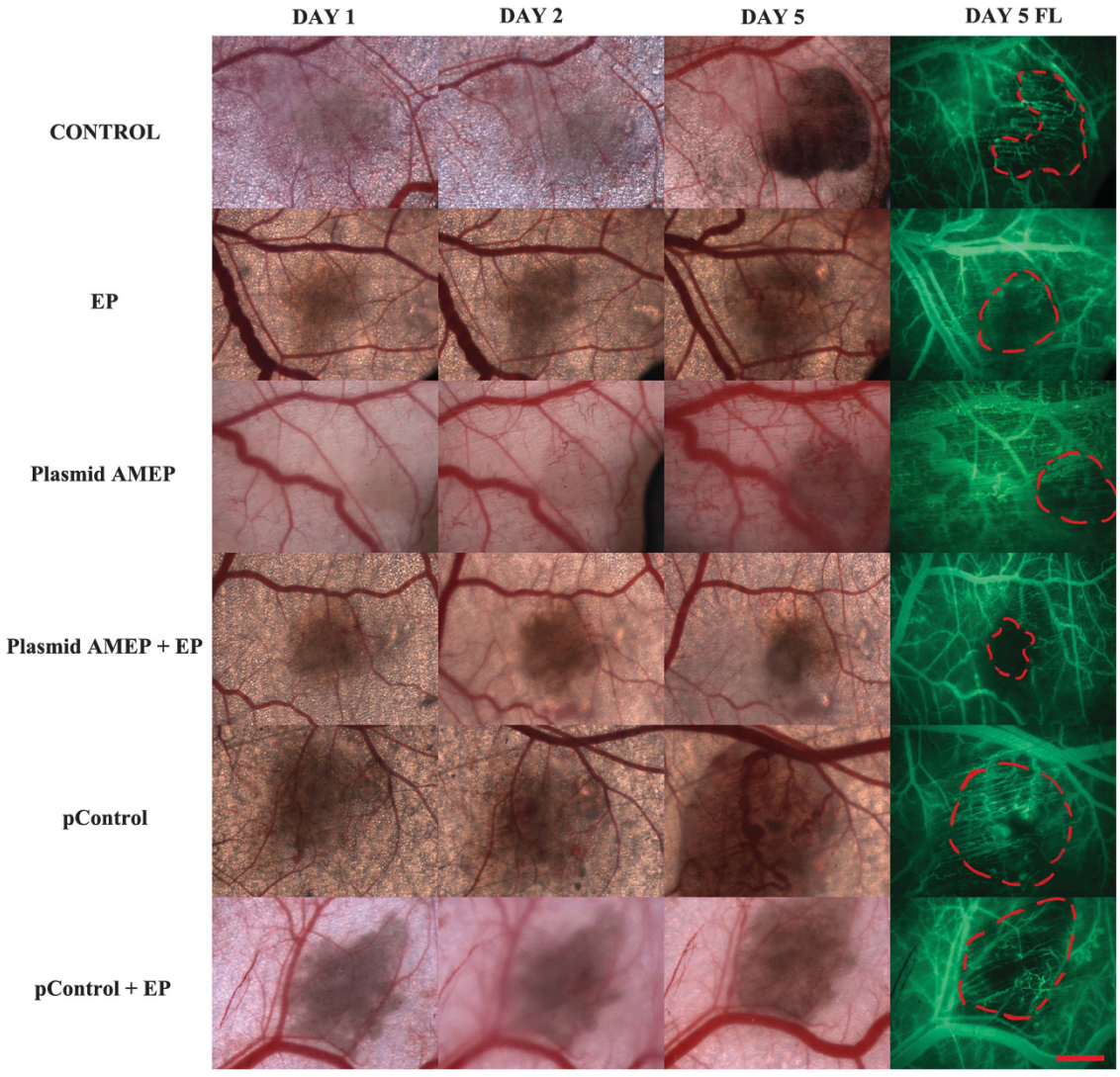

Figure 8. Intratumoral GET of Plasmid AMEP inhibited the formation of tumor blood vessels in B16F1 tumor in dorsal window chamber model. Bright-filed images of tumors and blood vessels in dorsal window chamber on the day of therapy (day 1), 1 day (day 2) and 4 days after the therapy (day 5) with GET of Plasmid AMEP, and fluorescence images of blood vessels (green) at day 5 (day 5 FL). Scale bar, 1 mm. Red dotted line on fluorescence images indicates the position of the tumor.

In vitro lipofection of plasmid DNA

One day before lipofection, 2×10^4 SVEC 4–10 cells were plated 24-well plates (Corning Inc., Corning, NY, USA) in order to reach 90% confluence. After 24 h, complexes of plasmid DNA (pEGFP, Plasmid AMEP) and Lipofectamine 2000 (Life Technologies) were prepared according to the manufacturer's instructions. After overnight incubation at 37 °C in a 5% CO_2 humidified incubator, cells were seeded for tube formation assay.

Proliferation assay

After GET, cells were plated on a 6-cm Petri dish (Corning) for 16 h to recover. Viable SVEC 4–10 (3×10^2) cells were plated for the proliferation assay in 0.1 ml of appropriate media in 96-well plates and incubated at 37 °C in a 5% CO_2 humidified incubator. Presto Blue assay was performed on days 0, 2 and 4, according to the manufacturer's instructions (LifeTechnologies). Proliferation of cells in each experimental group was normalized to day 0. To determine the numerical values of proliferation reduction at day 4, the additional normalization to the untreated control group at day 4 was performed. pEGFP was used as a control plasmid.

Adhesion assay

A cell adhesion assay was performed 2 days after GET to study the effect of Plasmid AMEP on endothelial cell attachment on basement membrane Precoated Matrigel plates (BD BioCoat BD Matrigel Matrix, thin layer, 96-well Microtest Plates, BD BioCoat), which were first rehydrated with warm FBS-free medium for 30 min. The nonspecific attachment was blocked with 0.5% bovine serum albumin (Sigma, St Louis, MO, USA) in FBS-free medium for 30 min. Afterwards, 2×10^4 viable SVEC 4–10 cells were plated in 0.1 ml of appropriate FBS-free media and incubated at 37 °C in a 5% CO_2 humidified incubator for 30 min. Each well was then washed twice with phosphate-buffered saline. Presto Blue assay was performed, to determine cell adhesion, according to the manufacturer's instructions. Adhesion of cells in each experimental group was normalized to the untreated control group.

Migratory and invasion potential assay

To determine the effect of plasmid AMEP on migration and invasion potential of endothelial cells, the bottoms of CIM-16 (Roche Diagnostics, Mannheim, Germany) topchambers were coated with 0.3 µg of human fibronectin (BD Biosciences) and incubated in a laminar air flow chamber for 30 min. The upper compartments of CIM-16 top chambers were then

© 2015 Macmillan Publishers Limited

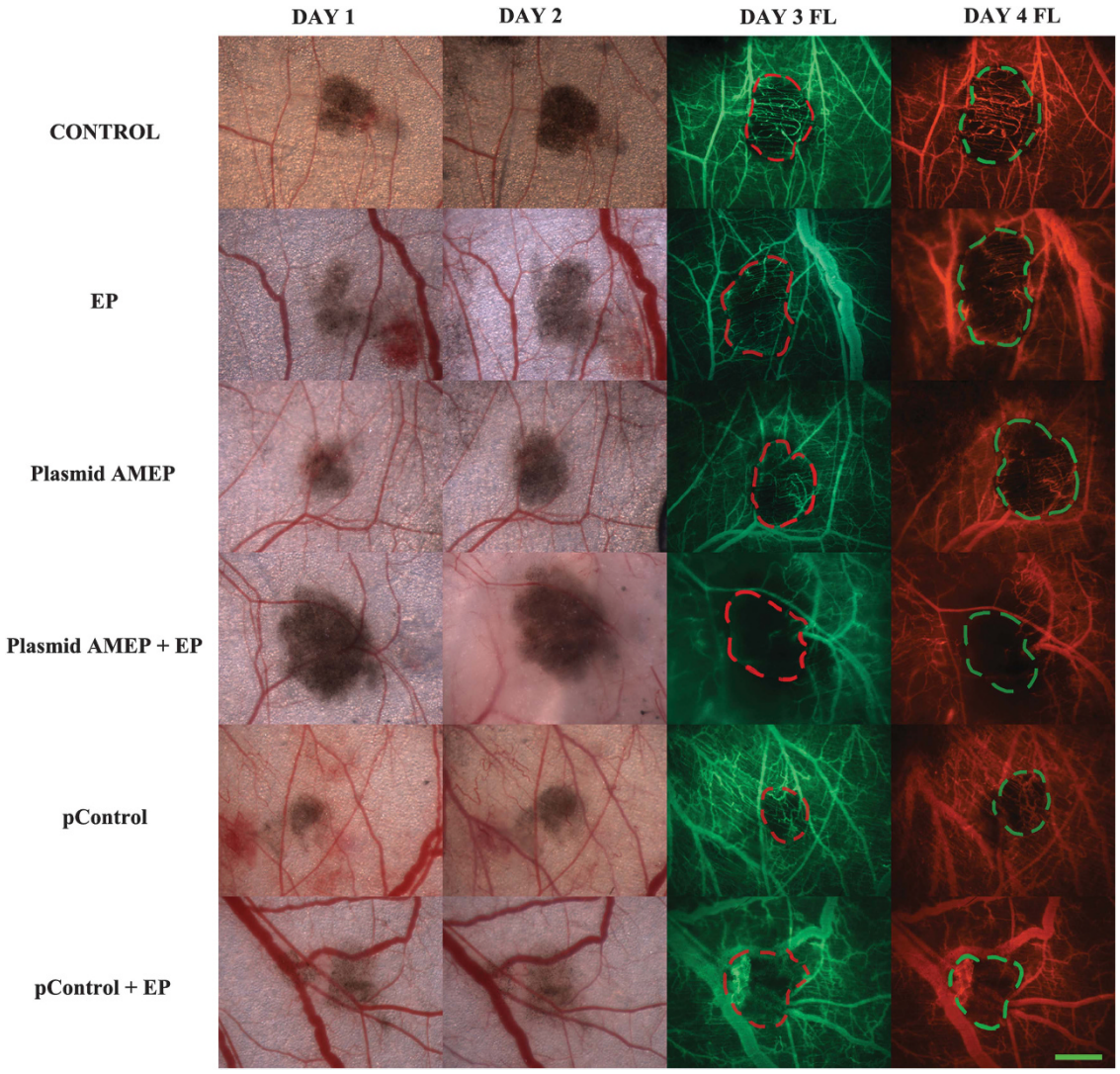

Figure 9. GET of Plasmid AMEP inhibited the formation of tumor blood vessels in B16F10 tumors in dorsal window chamber model. Bright-filed images of tumors and blood vessels in dorsal window chamber at the day of therapy (day 1), 1 day after the therapy (day 2) with GET of Plasmid AMEP and fluorescence images of blood vessels 2 days (green, day 3 FL) and 3 days (red, day 4 FL) after the therapy with GET of Plasmid AMEP. Scale bar, 1 mm. Red and green dotted lines on fluorescence images indicate the position of the tumor.

Table 3. Expression levels of mRNA for different proteins involved in integrin signaling pathway 24 h after GET of Plasmid AMEP

Group	*N*	*Talin*	*Vinculin*	*ilk*	*Rac*	*c-src*
B16F10 tumors						
Control	7	1.03 ± 0.11	1.28 ± 0.40	1.12 ± 0.21	1.03 ± 0.10	1.27 ± 0.40
EP	6	0.72 ± 0.10	0.49 ± 0.08	1.03 ± 0.10	0.98 ± 0.05	0.63 ± 0.17
Plasmid AMEP	6	1.00 ± 0.31	0.56 ± 0.13	1.25 ± 0.29	1.01 ± 0.19	0.64 ± 0.23
Plasmid AMEP+EP	7	**0.41 ± 0.10**	**0.40 ± 0.18**	**0.72 ± 0.15**	**0.62 ± 0.12**	**0.38 ± 0.09**
pControl	6	1.52 ± 0.38	1.09 ± 0.29	0.88 ± 0.14	1.31 ± 0.38	0.62 ± 0.19
pControl+EP	7	1.05 ± 0.24	0.72 ± 0.13	1.37 ± 0.35	1.04 ± 0.22	0.77 ± 0.24

Abbreviations: AMEP, antiangiogenic metargidin peptide; EP, electroporation; GET, gene electrotransfer. *N* (number of mice in each group).

coated with 0.5 μg of human fibronectin for the migration assay or thick layer (20 μl per membrane) of 0.75 mg ml^{-1} Matrigel (BD Bioscience) for the invasion assay, prepared in appropriate FBS-free media, respectively. Coated CIM plates were incubated at 37 °C in a 5% CO_2 for 2 h. After 2 h, the upper compartments were washed with 50 μl of phosphate-buffered saline, only for migratory assay. The bottom chambers were filled with 180 μl of corresponding media containing FBS. The top and bottom chambers of the CIM-16 plates were assembled together, 80 μl of FBS-free media was added to the top chamber and CIM-16 plates were allowed to equilibrate for 10 min at 37 °C, 5% CO_2 before the addition of cells. GET of SVEC 4–10 cells was performed 16 h before seeding. Eighty μl of viable 1×10^4 SVEC 4–10 cells per well for migration assay and 2×10^4 SVEC 4–10

© 2015 Macmillan Publishers Limited

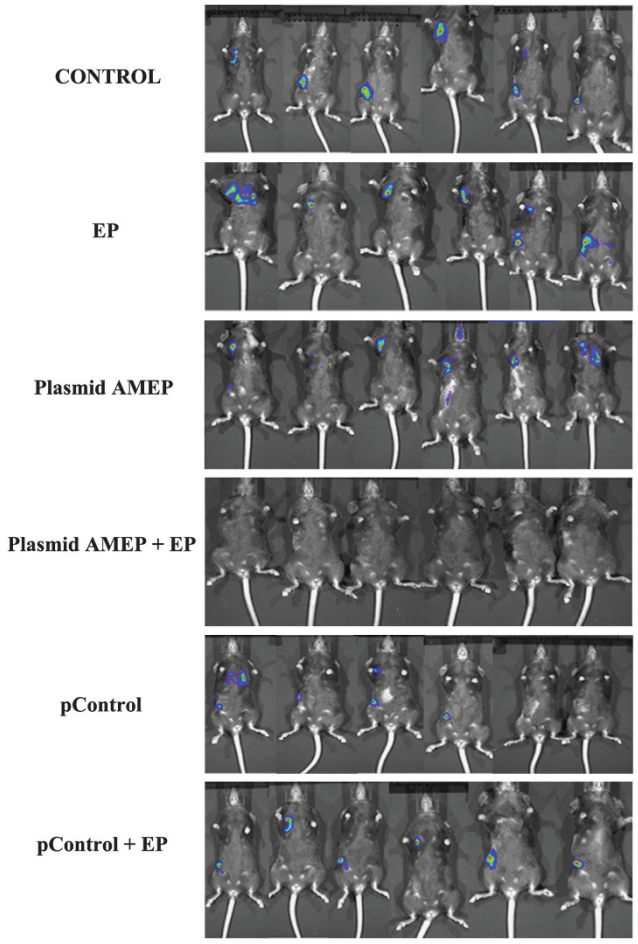

Figure 10. Development of lymphoid or lung metastases after GET of Plasmid AMEP. Imaging was performed with a Perkin Elmer IVIS Spectrum system. Luciferase signals from the surface of the representative mice (two from triplicate repeated experiments) are shown.

Table 4. Development of distant metastases after GET of Plasmid AMEP in highly metastatic murine melanoma B16F10 tumor model

Group	*Number of metastases free mice/all mice*	*Metastases-free mice (%)*
Control	3/12	25 ± 0
EP	3/12	25 ± 14
Plasmid AMEP	6/12	50 ± 14
Plasmid AMEP+EP	**11/12**	**92 ± 8***
pControl	5/12	42 ± 8
pControl+EP	7/12	58 ± 8

Abbreviations: AMEP, antiangiogenic metargidin peptide; EP, electroporation; GET, gene electrotransfer. Results represent three independent experiments, $n = 4$ for each experimental group in each experiment and are expressed as mean ± s.e. *$P < 0.05$ vs all groups.

cells per well for invasion assay were seeded into the top chambers of CIM-16 plates and placed into the xCELLigence Real Time Cell Analyzer (Roche Diagnostics) for data collection. Every 15 min during the following 72 h impendence data, reported as cell index, were collected with the xCELLigence software. The migration and invasion of cells were shown as a curve in a two-dimensional system (time, cell index), where only the linear part of the curve was considered for the analysis. The percentage of migration and invasion was calculated by the ratio of the slope of migrated/invaded treated cells to the slope of migrated/invaded untreated control cells.

Tube formation assay

A tube formation assay was performed to determine the effect of plasmid AMEP on the capability of murine endothelial cells to form capillary like structures *in vitro*. Two days after GET or 1 day after lipofectamine delivery, 2×10^4 viable SVEC 4–10 cells were plated on µ-Slide Angiogenesis (Ibidi, Munich, Germany) coated with Matrigel as described previously and incubated for 2–3 h until tubular complexes were formed. These complexes were stained with Calcein AM (Sigma). Images were captured with a DP72 CCD camera (Olympus, Hamburg, Germany) connected to an IX-70 inverted microscope. AxioVision program (Carl Zeiss, Jena, Germany) was used to convert raw images into binary masks, which were quantified with AngioQuant image analysis program[33]. The number of tubular complexes was determined for each experimental group and normalized to the number of complexes of untreated control group. One tubular complex is defined as all connected capillary like structures. The more organized the capillary-like structures are, the less tubular complexes are formed.

Animals and tumors

Female C57Bl/6 mice, 6–8-week old, purchased from Harlan Laboratories (Udine, Italy), were used in the study. Before the experiment, mice were subjected to an adaptation period of 2 weeks. Animals were maintained under specific pathogen-free conditions at a constant room temperature, humidity and a 12-h light/dark cycle. Food and water were provided *ad libitum*. Animal studies were carried out in accordance with the guidelines for animal experiments of the EU directives and the permission from the Veterinary Administration of Ministry of Agriculture and the Environment of the Republic of Slovenia (permission No.: 34401-4/2012/4). For induction of subcutaneous tumors, a suspension of 1×10^6 B16F1 or B16F10 cells in 0.1 ml of physiological saline was injected into the right flank. Animals were randomly divided into experimental groups and subjected to a specific experimental protocol when the largest tumor diameter reached 3 mm.

In vivo GET of plasmid DNA into subcutaneous tumors and leg muscle

Intratumoral GET. On days 0 and 2, 25 µl of Plasmid AMEP (100 µg), pControl (100 µg) or endotoxin-free water were injected into the tumors. Ten minutes after the injection, eight square electric pulses with a voltage-to-distance ratio of 600 V cm^{-1}, a pulse duration of 5 ms and a frequency 1 Hz were applied. Electric pulses were generated by electric pulse generator ELECTRO CELL B10 (Betatech, L'Union, France) and delivered through two parallel stainless steel electrodes with 2 or 4 mm distance between them, depending on the tumor volume. After four pulses, electrodes were turned for 90° for four additional pulses to assure GET of entire tumor.

Intramuscular GET. On days −3 and −1day before induction of subcutaneous tumors, hair was removed from the leg using depilation cream (Veet Sensitive Skin, Reckitt Benckiser, Slough, UK) before treatment. Plasmids or water were injected into the tibialis cranialis muscle, each time into a different leg. Experiment was performed with two different Plasmid AMEP doses (50 and 200 µg) in 50 µl. Afterwards, the leg was placed between the parallel stainless steel electrodes coated with conductive gel (Ultraschall Gel, P.J. Dahlhausen, & Co. GmbH, Koln, DE) to assure good contact between electrodes and overlying skin at a 6 mm distance. The combination of one high voltage (voltage-to-distance ratio 600 V cm^{-1}, pulse duration 100 µs, frequency 1 Hz) and four low voltage pulses (voltage-to-distance ratio 80 V cm^{-1}, pulse duration 100 ms, frequency 1 Hz) was applied by an electric pulse generator (Cliniporator, IGEA s.r.l., Carpi, Italy). There was a 1-s pause between high and low-voltage pulses and after second low-voltage pulses electrodes were turned for 180 degrees.

Tumor growth

To determine the antitumor effect of Plasmid AMEP on the growth of subcutaneous B16F1 and B16F10 melanoma tumors, tumor volume was

© 2015 Macmillan Publishers Limited

Table 5. Primer sequences for proteins involved in integrin-linked signaling pathway

	Forward (sense)	*Reverse (antisense)*
Talin	5′-GAGAAGACCAAGGAGGTGATTC-3′	5′-GCCATCCTGATAGTCTCCAAAG-3′
Vinculin	5′-ACCTTGAACAGCTACGACTAAC-3′	5′-CAGGGAACTCTTCATCCTTCTC-3′
ilk	5′-GCCACTTCACTATGCATGTTTC-3′	5′-CAGGCATCTCTCCATACTTGTT-3′
rac	5′-GGGATGATAAGGACACCATTGA-3′	5′-GCTGAGCACTCCAGGTATTT-3′
c-src	5′-CGAGTGCCTTACCCAAGAAT-3′	5′-CAGTTCTTCATCACCTCGTAGAC-3′
β-actin	5′-GAAGTGTGACGTTGACATCC-3′	5′-ACTCATCGTACTCCTGCTTG-3′
GAPDH	5′-TTCACCACCATGGAGAAGGC-3′	5′-GGCATGGACTGTGGTCATGA-3′

measured every second day after the therapy using digital Vernier caliper. The volume was calculated according to the formula for ellipsoid: $V = a \times b \times c \times \pi/6$, where *a*, *b* and *c* represent perpendicular tumor diameters. The growth delay, the difference in time when treated and untreated tumors reach a tumor volume of 40 mm^3 was determined. Each experimental group consisted of 12–18 mice. The weight of the mice was followed as a general index of systemic toxicity.

Histology

Three days after the second therapy, four mice from each experimental group were killed. The tumors were excised and fixed in IHC zinc fixative (BD Pharmingen, BD Biosciences) overnight. Afterwards, they were embedded in paraffin and four consecutive 2-µm thick sections were cut from each paraffin block. The first section of each tumor sample was stained with hematoxylin and eosin. The remaining sections were immunohistochemically stained with rabbit polyclonal antibodies against CD31 (ab28364, Abcam, Cambridge, MA, USA) at dilution 1:1000, rabbit monoclonal antibodies against Ki-67 (clone SP6, Thermo Fisher Scientific, Cambridge, MA, USA) at dilution 1:1200 and rabbit monoclonal antibodies against Cleaved Caspase-3 (Ca-3, Cell Signalling Technology, Danvers, MA, USA) at dilution 1:1500. A peroxidase-conjugated streptavidin–biotin system (Rabbit specific HRP/DAB detection IHC kit, ab64261, Abcam) was used as the colorogenic reagent followed by hematoxylin counterstaining. The images of immunohistochemically stained sections were captured with a DP72 CCD camera (Olympus) connected to a BX-51 microscope (Olympus). From each slide, five images of viable tumor tissue were analyzed under the light microscopy. The number of CD31-positive blood vessels was determined on the acquired images. Three independent observers blinded to the treatment groups quantified the percentage of tumor necrosis and the number of Ki-67- or Ca-3-positive cells.

Total mRNA extraction and qRT-PCR analysis

AMEP mRNA expression. RNA extraction and qRT-PCR analysis were performed 3 days after the second therapy to determine AMEP expression in murine melanoma tumors. This time period was chosen based on a previous *in vitro* data[7]. Mice were killed and five tumors from each experimental group were excised and frozen in liquid nitrogen. Tumors were later homogenized in a mortar with a pestle and total RNA was extracted with the TRIzol Plus RNA Purification System (Life Techmologies) according to the manufacturer's instructions. Concentrations and purity of RNA was determined spectrophotometrically (Epoch, Biotek, Winooski, VT, USA). cDNA transcription was performed on 500 ng of total RNA extract using the SuperScript VILO cDNA Synthesis Kit (Life Techmologies), according to the manufacturer's instructions. For the quantitative polymerase chain reaction (qPCR), 10-fold diluted mixtures of transcribed cDNA were used as a template using TaqMan Gene Expression Master Mix (Life Technologies) and TaqMan Gene Expression Assay (Applied Biosystems, Life Technologies). Custom primers and TaqMan probe sequence (forward primer sequence: 5′-GGCCAGGTGCACAGTGT-3′, reverse primer sequence: 5′-AGACGGGCGCAGCT-3′) were designed to amplify the fragment of human AMEP cDNA; to amplify human or murine 18 S ribosomal RNA, TaqMan probes (Hs00172187_m1 and Mm03928990_g1) were used as an internal control. qPCR was performed on 7300 System (Applied Biosystems) and products were later analyzed with associated 7300 System SDS software. The thermal cycler protocol consisted of activation of Uracil-DNA Glycosylase (2 min at 50 °C), hot start activation of AmpliTaq Gold Enzyme (10 min at 95 °C), 45 cycles of denaturation (15 s at 95 °C), annealing and extension (1 min 60 °C). Relative quantification of the qPCR data was performed by the $2^{-\Delta\Delta Ct}$ method.[34]

Expression of integrin signaling pathway. Mice with subcutaneous tumors were killed at 4, 24 and 60 h after the first therapy. Tumors were excised and processed as described above. Afterwards, the total mRNA was extracted and qRT-PCR was performed for several specific genes involved in integrin-linked angiogenesis signaling pathway (Table 5). The qPCR and the analysis of the qPCR data was performed using Power SYBR Green master mix (Applied Biosystems) on a CFX-96 Real-Time PCR Detection system (Bio-Rad, Hercules, CA, USA). Relative quantification of cDNA expression was normalized to β-actin and GAPDH by the $2^{-\Delta\Delta Ct}$ method.[34]

Dorsal window chamber

For the implantation of the dorsal window chamber, mice were first anesthetized with an intraperitoneal injection of anesthetic mixture consisting of ketamine (1 mg ml^{-1}, Narketan; Vetoquinol, Ittigen, Switzerland), xylazine (5 mg ml^{-1}, Chanazine; Chanelle Pharmaceuticals, Loughrea, Ireland) and acepromazine (0.4 mg ml^{-1}, Promace; Fort Dodge Animal Health, USA). Heating pads were used to keep animals warm and an aseptic technique was used throughout the entire surgical procedure. The hair at the back of the mouse was completely removed by shaving followed by depilatory cream (Vitaskin, Krka, Novo Mesto, Slovenia). Afterwards, the dorsal window chamber (APJ Trading, Ventura, CA, USA) consisting of two titanium frames was surgically implanted onto the extended double layer of the skin with stainless-steel screws and sutures. One layer of the skin was excised to expose the vasculature of the lower layer of the skin. To ensure optimal microscopic observation and image capturing, all the fat and connective tissues were dissected from the lower layer of the skin. The dorsal window chamber was filled with physiological solution and closed with a 12-mm cover glass (Glaswarenfabrik Karl Hecht, Sondheim, Germany). To avoid post-surgical pain, butorphanol (0.3 mg kg^{-1}, Torbugesic; Fort Dodge Animal Health) was injected intramuscularly immediately after the surgery and the following day. A suspension of 3.5×10^5 B16F1 or B16F10 melanoma cells in 5 µl of physiological saline was injected into the lower layer of the skin when mice totally recovered from the surgery. The next day, when tumor blood vessels began to develop, 5 µl of Plasmid AMEP (20 µg), pControl (20 µg) or endotoxin-free water were injected into the tumors. Parallel experimental groups were treated with injection alone and in combination with electric pulses. The pulses were delivered immediately after the intratumoral injection through two parallel stainless steel electrodes with 4-mm distance. Eight square-wave pulses, generated by ELECTRO CELL B10, in two sets of four pulses in perpendicular directions with voltage-to-distance ratio 600 V cm^{-1}, pulse duration 5 ms and frequency 1 Hz were applied. Dorsal window chambers were monitored for 4 (B16F10) or 5 (B16F1) days with intravital microscopy using a Carl Zeiss SteREO Lumar.V12 fluorescence stereomicroscope equipped with a NeoLumar S 0.86 objective and a MRc5 digital camera (Carl Zeiss). The animals were anesthetized by inhalation (1, 5% Isoflurane, Nicholas Piramal India Ltd.) and placed on a custom-designed holder. Bright-field images of window chambers were taken every 24 h. On days 3 (B16F10) or 5 (B16F1) after tumor induction, blood vessels were stained with intravenous injection of FITC dextran (70 kDa; Sigma) and additionally stained with Rhodamine B (70 kDa, Sigma) on day 4 (B16F10) and images of fluorescent blood vessels were captured.

Bioluminescence imaging for detection of metastases

To evaluate the antimetastatic activity of AMEP after GET of Plasmid AMEP, luminescent 1.1×10^6 B16-F10-luc-G5 cells were implanted on the flank. Five days after the first day of therapy, tumors were surgically excised and the development of metastases was monitored weekly. Ten minutes before image acquisition, 150 mg kg^{-1} of luciferin was injected

© 2015 Macmillan Publishers Limited

intraperitoneally and the luminescent signal was acquired using a Perkin Elmer IVIS Spectrum system (Caliper, Life Sciences, Waltham, MA, USA). When metastases were detected, mice were humanely euthanized.

Statistical analysis

All data were tested for normality of distribution with the Shapiro–Wilk test. The differences between the experimental groups were statistically evaluated by one-way analysis of variance followed by a Holm–Sidak test for multiple comparison. A *P*-value of < 0.05 was considered to be statistically significant. SigmaPlot Software (Systat Software, Chicago, IL, USA) was used for statistical analysis and graphical representation.

CONFLICT OF INTEREST

CB is a stockholder and an employee at ONXEO. The remaining authors declare no conflict of interest.

ACKNOWLEDGEMENTS

We acknowledge the financial support from the state budget by the Slovenian Research Agency (programs no. P3-0003 and P1-0140 and projects no. J3-4211, J3-4259). The research was conducted in the scope of LEA EBAM (French-Slovenian European Associated Laboratory: Pulsed Electric Fields Applications in Biology and Medicine) and is a result of networking efforts within COST TD1104 Action. We thank Mira Lavric, Ursa Lampreht and Natasa Tesic (Institute of Oncology Ljubljana, Ljubljana, Slovenia) and Miha Butinar (Jozef Stefan Institute) for all the valuable work they contributed to this research.

REFERENCES

1 Heller LC, Heller R. Electroporation gene therapy preclinical and clinical trials for melanoma. *Curr Gene Ther* 2010; **10**: 312–317.
2 Daud AI, DeConti RC, Andrews S, Urbas P, Riker AI, Sondak VK *et al.* Phase I trial of interleukin-12 plasmid electroporation in patients with metastatic melanoma. *J Clin Oncol* 2008; **26**: 5896–5903.
3 Cemazar M, Jarm T, Sersa G. Cancer electrogene therapy with interleukin-12. *Curr Gene Ther* 2010; **10**: 300–311.
4 Mizejewski GJ. Role of integrins in cancer: survey of expression patterns. *Proc Soc Exp Biol Med* 1999; **222**: 124–138.
5 Trochon-Joseph V, Martel-Renoir D, Mir LM, Thomaidis A, Opolon P, Connault E *et al.* Evidence of antiangiogenic and antimetastatic activities of the recombinant disintegrin domain of metargidin. *Cancer Res* 2004; **64**: 2062–2069.
6 Daugimont L, Vandermeulen G, Defresne F, Bouzin C, Mir LM, Bouquet C *et al.* Antitumoral and antimetastatic effect of antiangiogenic plasmids in B16 melanoma: higher efficiency of the recombinant disintegrin domain of ADAM 15. *Eur J Pharm Biopharm* 2011; **78**: 314–319.
7 Bosnjak M, Prosen L, Dolinsek T, Blagus T, Markelc B, Cemazar M *et al.* Biological properties of melanoma and endothelial cells after plasmid AMEP gene electrotransfer depend on integrin quantity on cells. *J Membr Biol* 2013; **246**: 803–819.
8 Spanggaard I, Snoj M, Cavalcanti A, Bouquet C, Sersa G, Robert C *et al.* Gene electrotransfer of plasmid antiangiogenic metargidin peptide (AMEP) in disseminated melanoma: safety and efficacy results of a phase I first-in-man study. *Hum Gene Ther Clin Dev* 2013; **24**: 99–107.
9 Tesic N, Cemazar M. *In vitro* targeted gene electrotransfer to endothelial cells with plasmid DNA containing human endothelin-1 promoter. *J Membr Biol* 2013; **246**: 783–791.
10 Bosnjak M, Lorente BC, Pogacar Z, Makovsek V, Cemazar M. Different incubation times of cells after gene electrotransfer in fetal bovine serum affect cell viability, but not transfection efficiency. *J Membr Biol* 2014; **247**: 421–428.
11 Tevz G, Kranjc S, Cemazar M, Kamensek U, Coer A, Krzan M *et al.* Controlled systemic release of interleukin-12 after gene electrotransfer to muscle for cancer gene therapy alone or in combination with ionizing radiation in murine sarcomas. *J Gene Med* 2009; **11**: 1125–1137.
12 Mir LM, Banoun H, Paoletti C. Introduction of definite amounts of nonpermeant molecules into living cells after electropermeabilization: direct access to the cytosol. *Exp Cell Res* 1988; **175**: 15–25.
13 Mir LM, Orlowski S, Belehradek Jr. J, Paoletti C. Electrochemotherapy potentiation of antitumour effect of bleomycin by local electric pulses. *Eur J Cancer* 1991; **27**: 68–72.
14 Sersa G, Cemazar M, Miklavcic D. Antitumor effectiveness of electrochemotherapy with cis-diamminedichloroplatinum(II) in mice. *Cancer Res* 1995; **55**: 3450–3455.
15 Cemazar M, Miklavcic D, Sersa G. Intrinsic sensitivity of tumor cells to bleomycin as an indicator of tumor response to electrochemotherapy. *Jpn J Cancer Res* 1998; **89**: 328–333.
16 Jaroszeski MJ, Dang V, Pottinger C, Hickey J, Gilbert R, Heller R. Toxicity of anticancer agents mediated by electroporation *in vitro*. *Anticancer Drugs* 2000; **11**: 201–208.
17 Sersa G, Miklavcic D. Electrochemotherapy of tumours. *J Vis Exp* 2008; **15**: 1038.
18 Sedlar A, Dolinsek T, Markelc B, Prosen L, Kranjc S, Bosnjak M *et al.* Potentiation of electrochemotherapy by intramuscular IL-12 gene electrotransfer in murine sarcoma and carcinoma with different immunogenicity. *Radiol Oncol* 2012; **46**: 302–311.
19 Teissie J, Escoffre JM, Paganin A, Chabot S, Bellard E, Wasungu L *et al.* Drug delivery by electropulsation: Recent developments in oncology. *Int J Pharm* 2012; **423**: 3–6.
20 Edhemovic I, Brecelj E, Gasljevic G, Marolt Music M, Gorjup V, Mali B *et al.* Intraoperative electrochemotherapy of colorectal liver metastases. *J Surg Oncol* 2014; **110**: 320–327.
21 Miklavcic D, Mali B, Kos B, Heller R, Sersa G. Electrochemotherapy: from the drawing board into medical practice. *Biomed Eng Online* 2014; **13**: 29.
22 Mali B, Miklavcic D, Campana LG, Cemazar M, Sersa G, Snoj M *et al.* Tumor size and effectiveness of electrochemotherapy. *Radiol Oncol* 2013; **47**: 32–41.
23 Rols MP, Delteil C, Golzio M, Dumond P, Cros S, Teissie J. *In vivo* electrically mediated protein and gene transfer in murine melanoma. *Nat Biotechnol* 1998; **16**: 168–171.
24 Jaroszeski MJ, Gilbert R, Nicolau C, Heller R. *In vivo* gene delivery by electroporation. *Adv Drug Deliv Rev* 1999; **35**: 131–137.
25 Golzio M, Rols MP, Teissie J. *In vitro* and *in vivo* electric field-mediated permeabilization, gene transfer, and expression. *Methods* 2004; **33**: 126–135.
26 Vidic S, Markelc B, Sersa G, Coer A, Kamensek U, Tevz G *et al.* MicroRNAs targeting mutant K-ras by electrotransfer inhibit human colorectal adenocarcinoma cell growth *in vitro* and *in vivo*. *Cancer Gene Ther* 2010; **17**: 409–419.
27 Chabot S, Pelofy S, Paganin-Gioanni A, Teissie J, Golzio M. Electrotransfer of RNAi-based oligonucleotides for oncology. *Anticancer Res* 2011; **31**: 4083–4089.
28 Dolinsek T, Markelc B, Sersa G, Coer A, Stimac M, Lavrencak J *et al.* Multiple delivery of siRNA against endoglin into murine mammary adenocarcinoma prevents angiogenesis and delays tumor growth. *PLoS One* 2013; **8**: e58723.
29 Kamensek U, Sersa G, Cemazar M. Evaluation of p21 promoter for interleukin 12 radiation induced transcriptional targeting in a mouse tumor model. *Mol Cancer* 2013; **12**: 136.
30 Prosen L, Markelc B, Dolinsek T, Music B, Cemazar M, Sersa G. Mcam silencing with RNA interference using magnetofection has antitumor effect in murine melanoma. *Mol Ther Nucleic Acids* 2014; **3**: e205.
31 Crokart N, Danhier F, Daugimont L, Goncalves N, Jordan BF, Gregoire V *et al.* Potentiation of radiotherapy by a localized antiangiogenic gene therapy. *Radiother Oncol* 2013; **107**: 252–258.
32 Robinson SD, Hodivala-Dilke KM. The role of beta3-integrins in tumor angiogenesis: context is everything. *Curr Opin Cell Biol* 2011; **23**: 630–637.
33 Niemisto A, Dunmire V, Yli-Harja O, Zhang W, Shmulevich I. Robust quantification of *in vitro* angiogenesis through image analysis. *IEEE Trans Med Imaging* 2005; **24**: 549–553.
34 Livak KJ, Schmittgen TD. Analysis of relative gene expression data using real-time quantitative PCR and the 2(-Delta Delta C(T)) Method. *Methods* 2001; **25**: 402–408.

Supplementary Information accompanies this paper on Gene Therapy website (http://www.nature.com/gt)

© 2015 Macmillan Publishers Limited